Magnitudes and Orientations of the Principal Elements of the ^{1}H Chemical Shift, ^{1}H−^{15}N Dipolar Coupling, and ^{15}N Chemical Shift Interaction Tensors in $^{15}N_{\epsilon 1}$-Tryptophan and $^{15}N_{\pi}$-Histidine Side Chains Determined by Three-Dimensional Solid-State NMR Spectroscopy of Polycrystalline Samples

A. Ramamoorthy, C. H. Wu, and S. J. Opella*

Contribution from the Department of Chemistry, University of Pennsylvania, Philadelphia, Pennsylvania 19104

Received September 17, 1996. Revised Manuscript Received June 1, 1997[⊗]

Abstract: The magnitudes and orientations of the principal elements of the ^{1}H chemical shift, ^{1}H−^{15}N dipolar coupling, and ^{15}N chemical shift interaction tensors in $^{15}N_{\epsilon 1}$-tryptophan and $^{15}N_{\pi}$-histidine nitrogen sites were determined by the analysis of three-dimensional powder patterns obtained from ^{15}N-labeled powder samples of the amino acids. Although the magnitudes of the principal elements of the ^{1}H and ^{15}N chemical shift tensors for these two sites are quite different, their molecular orientations in the molecular frame are very similar. The least shielded ^{15}N chemical shift tensor element, σ_{33N}, and the most shielded ^{1}H chemical shift tensor element, σ_{11H}, are approximately colinear with the N−H bond in both cases. The principal elements, σ_{22H} and σ_{22N}, are in the plane of the indole ring for tryptophan and in the plane of the imidazole ring for histidine but oppose each other. σ_{11N} and σ_{33H} are perpendicular to the planes of these heterocyclic rings. The chemical shift tensors of the ^{1}H and ^{15}N nuclei in these two side chain nitrogen sites are distinctly different from those of backbone amide nitrogen sites.

Introduction

Although the anisotropic characteristics of the chemical shift and heteronuclear dipolar nuclear spin interactions influence the results of nearly all solution and solid-state NMR experiments, their effects can be most directly and simply observed in high-resolution solid-state NMR spectra of uniaxially oriented and single-crystalline and polycrystalline samples.[1−7] Since both the magnitudes and orientations of the principal elements of these tensors are required for the interpretation of spectroscopic results, as well as to obtain information about molecular structure and dynamics, determinations of the tensors have generally required detailed studies of single crystals. We have recently developed a way to characterize these tensors in powder samples using three-dimensional solid-state NMR correlation spectroscopy.[5] Previously, we used this approach to simultaneously characterize the ^{1}H−^{15}N heteronuclear dipolar coupling of the ^{1}H and ^{15}N chemical shift tensors of a peptide bond.[5] In this paper, we describe its application to two key nitrogen sites in the side chains of the amino acids tryptophan and histidine

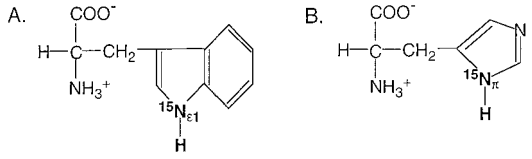

Figure 1. Chemical structures of (A) tryptophan and (B) histidine showing the ^{15}N sites.

(Figure 1). For both the indole nitrogen of tryptophan and the π nitrogen of histidine, the information about the ^{1}H chemical shift tensors is new. The ^{15}N chemical shift tensor of the π nitrogen of histidine has been determined by single-crystal experiments, and the comparison demonstrates the validity of our method with powder samples. The ^{15}N chemical shift tensor of the indole nitrogen of tryptophan has been analyzed,[3,4] but has not been determined because single crystals are unavailable. The results presented here resolve a discrepancy concerning the orientation of the tensor in the molecular frame by confirming that one of the principal element is aligned along the N−H bond axis.

The concepts and methods associated with selective averaging of nuclear spin interactions in solid-state NMR spectroscopy were invented, in large part, in order to be able to characterize chemical shift tensors.[1] While it is a simple matter to measure the magnitudes of the three principal elements of a chemical shift tensor (σ_{11}, σ_{22}, and σ_{33}) directly from the discontinuities observed in a powder pattern,[8,9] this typically provides no information about the orientation of the chemical shift tensor in the molecular frame. Traditionally, the only sure way to determine both magnitudes and orientations of the principal elements of a chemical shift tensor has been to perform a rotation study of a single crystal of a molecule whose structure has been determined by X-ray diffraction.[8,10,12,13] Much valu-

[⊗] Abstract published in *Advance ACS Abstracts*, October 15, 1997.

(1) (a) Waugh, J. S.; Huber, L. M.; Haeberlen, U. *Phys. Rev. Lett.* **1986**, *20*, 180−182. (b) Pines, A.; Gibby, M. G.; Waugh, J. S. *J. Chem. Phys.* **1973**, *59*, 569−590.

(2) Linder, M.; Hohener, A.; Ernst, R. R. *J. Chem. Phys.* **1980**, *73*, 4959−4970.

(3) Cross, T. A.; Opella, S. J. *J. Am. Chem. Soc.* **1983**, *105*, 306−308.

(4) Hu, W.; Lee, K.-C.; Cross, T. A. *Biochemistry* **1993**, *32*, 7035−7067.

(5) Wu, C. H.; Ramamoorthy, A.; Gierasch, L. M.; Opella, S. J. *J. Am. Chem. Soc.* **1995**, *117*, 6148−6149.

(6) (a) Smith, S. O.; Griffin, R. G. *Annu. Rev. Phys. Chem.* **1988**, *39*, 511−535. (b) Torchia, D. A. *Annu. Rev. Biophys.* **1984**, *13*, 124−144.

(7) (a) Shoji, A.; Ozaki, T.; Fujito, T.; Deguchi, K.; Ando, S.; Ando, I. *Macromolecules* **1989**, *22*, 2860−2863. (b) Shoji, A.; Ozaki, T.; Fujito, T.; Deguchi, K.; Ando, S.; Ando, I. *J. Am. Chem. Soc.* **1990**, *112*, 4693−4697. (c) Kuroki, S.; Asakawa, N.; Ando, S.; Ando, I.; Shoji, A.; Ozaki, T. *J. Mol. Struct.* **1991**, *245*, 69−80. (d) Shoji, A.; Ando, S.; Kuroki, S.; Ando, I.; Webb, G. A. In *Annual Reports on NMR Spectroscopy*; Webb, G. A., Ed.; Academic Press: London, 1993; Vol. *26*, pp 55−98.

(8) Harbison, G.; Herzfeld, J.; Griffin, R. G. *J. Am. Chem. Soc.* **1981**, *103*, 4752−4754.

S0002-7863(96)03267-2 CCC: $14.00

able information about chemical shift tensors, as well as other interactions, has been obtained in this way. However, these measurements can be tedious, and because they require large, high-quality single crystals, which can be difficult or impossible to obtain for many of the most interesting molecules, they are inherently limited to selected examples. Thus, there is considerable value in developing methods that utilize powder rather than single crystal samples for the determination of chemical shift tensors. This will enable examples of many more tensors to be characterized.

Solid-state NMR experiments that correlate chemical shift and dipolar coupling parameters in one[4,14−17] or two dimensions[2,18−22] have been used to characterize a number of different tensors in powder samples. These methods usually employ multiple pulse sequences, spatial averaging with magic angle sample spinning (MAS), or a combination of these to separate the effects from the two interactions.[18−24] One- and two-dimensional powder patterns can contain, in principle, sufficient information to determine the relative orientations of chemical shift and dipolar tensors in selected cases.

However, higher dimensional experiments enable more accurate determinations to be performed. The frequencies characterizing the interactions are separated through placement along different axes. The tensors from multiple sites can be analyzed independently.[5,25] Once the magnitudes and orientations of the principal elements of the tensors are established, they can be utilized in solid-state NMR structural studies of uniaxially oriented systems[26] among other applications, including the analysis of relaxation measurements in solution NMR spectroscopy.

The indole side chain of tryptophan appears to play a vital role in membrane proteins through interactions at the hydrophobic−hydrophilic interface of lipid bilayers.[3,27,28] Solid-state NMR studies have been performed on tryptophan to understand its role in the ion-channel activity of gramicidin in membrane environments through the measurement of spin interaction tensors pertaining to the indole ring.[4] Much of the background for interpretation of both solution and solid-state NMR results on Trp residues in proteins has come from solid-state NMR studies of selected systems. Cross and Opella determined the orientation of the N−H bond of the single tryptophan residue in the coat protein of oriented bacteriophage fd[3] from the $^{1}H-^{15}N$ dipolar coupling measured with a two-dimensional ^{15}N chemical shift/$^{1}H-^{15}N$ dipolar coupling experiment. Cornell et al.[27] and Separovic et al.[28] studied the ^{13}C chemical shift and $^{13}C-^{14}N_{\epsilon 1}$ dipolar tensors associated with the $^{14}N_{\epsilon 1}-^{13}C_{\delta 1}$ bond of the indole ring of the tryptophan residue in gramicidin. Hu et al.[4] examined the ^{15}N chemical shift and $^{15}N_{\epsilon 1}-^{2}H$ dipolar coupling tensors of tryptophan through the analysis of the one-dimensional ^{15}N chemical shift powder patterns by taking the ^{2}H quadrupole interaction into account.

Histidine residues are the focus of attention in many studies of the mechanisms of action of enzymes because of the essential chemical roles for the imidazole side chains.[29] Resonance frequencies of the ^{1}H, ^{13}C, and ^{15}N nuclei in the imidazole group change as a function of pH. Titration is in "slow exchange" in the solid state in contrast to the "fast exchange" observed in solution.[30−32] The solid-state NMR properties of histidine alone and in a protein have been described by Griffin and coworkers.[11,32,33] The isotropic and anisotropic chemical shifts of ^{15}N at the π position of the imidazole ring were found to be sensitive to tautomeric structure, the protonation state, and hydrogen bonding interactions.[32] Harbison et al.[8] characterized the ^{15}N chemical shift tensors at the π and τ sites of the imidazole ring of histidine using solid-state NMR experiments on a single-crystal sample. Later, Munowitz et al.[32] studied the acid−base and tautomeric equilibria of a histidine powder sample using one-dimensional MAS experiments. They were able to separate the ^{15}N powder patterns from the protonated and nonprotonated forms of the histidine molecule based on the $^{1}H-^{15}N$ dipolar couplings and were able to explain the changes in the isotropic chemical shift of $^{15}N_{\pi}$ due to hydrogen bonding.

Experimental Section

All of the NMR experiments were performed on a home-built spectrometer with a 12.9 T wide-bore Magnex 550/89 magnet with resonance frequencies of 55.7 and 550.09 MHz for ^{15}N and ^{1}H, respectively. The powder samples in sealed glass tubes were placed within a 5 mm solenoidal coil double-tuned to the ^{1}H and ^{15}N resonance frequencies in a home-built probe. The 50-mg $^{15}N_{\epsilon 1}$-tryptophan and 80-mg $^{15}N_{\pi}$-histidine samples were obtained from Cambridge Isotope Laboratories (Andover, MA). The magnitudes of the principal elements and the isotropic chemical shift of the indole nitrogen of tryptophan sample were consistent with there being a single species present and the values observed for tryptophan residues in peptides and proteins.

(9) (a) Power, W. P.; Wasylishen, R. E. *Annu. Rep. NMR Spectrosc.* **1991**, *23*, 1−84. (b) Wasylishen, R. E.; Curtis, R. D.; Eichele, K.; Lumsden, M. D.; Penner, G. H.; Power, W. P.; Wu, G. *Nuclear Magnetic Shielding and Molecular Structure*; NATO ASI Series C.; Tossell, J. A., Ed.; Kluwer Academic Publishers: Dordrecht, 1993; Vol. *368*, pp 297−314. (c) Fenzke, D.; Hunger, M.; Pfeifer, H. *J. Magn. Reson.* **1991**, *95*, 477−483. (d) Yeo, J. H.; Demura, M.; Asakura, T.; Fujito, T.; Imanari, M.; Nicholson, L. K.; Cross, T. A. *Solid State Nucl. Magn. Reson.* **1994**, *3*, 209−218.

(10) Tegenfeldt, J.; Feucht, H.; Ruschitzka, G.; Haeberlen, U. *J. Magn. Reson.* **1980**, *39*, 509−520.

(11) Duncan, T. M. *A Compilation of Chemical Shift Anisotropies*; The Farragut Press: Chicago, 1990.

(12) Harbison, G. S.; Jelinski, L. W.; Stark, R. E.; Torchia, D. A.; Herzfeld, J.; Griffin, R. G. *J. Magn. Reson.* **1984**, *60*, 79−82.

(13) Gerald, R., II; Bernhard, T.; Haeberlen, U.; Rendell, J.; Opella, S. J. *J. Am. Chem. Soc.* **1993**, *115*, 777−782.

(14) Hartzell, C. J.; Whitfield, M.; Oas, T. G.; Drobny, G. P. *J. Am. Chem. Soc.* **1987**, *109*, 5966−5969.

(15) Hiyama, Y.; Niu, C.-H.; Silverton, J. V.; Bavoso, A.; Torchia, D. A. *J. Am. Chem. Soc.* **1988**, *110*, 2378−2383.

(16) Teng, Q.; Cross, T. A. *J. Magn. Reson.* **1989**, *85*, 439−447.

(17) Lumsden, M. D.; Wasylishen, R. E.; Eichele, K.; Schindler, M.; Penner, G. H.; Power, W. P.; Curtis, R. D. *J. Am. Chem. Soc.* **1994**, *116*, 1403−1413.

(18) Munowitz, M. G.; Griffin, R. G. *J. Chem. Phys.* **1982**, *76*, 2848−2858.

(19) Frey, M. H.; DiVerdi, J. A.; Opella, S. J. *J. Am. Chem. Soc.* **1985**, *107*, 7311−7315.

(20) Schmidt-Rohr, K.; Wilhelm, M.; Hohansson, A.; Spiess, H. W. *Magn. Reson. Chem.* **1993**, *31*, 352−356.

(21) (a) Nakai, T.; Ashida, J.; Terao, T. *J. Chem. Phys.* **1988**, *88*, 6049−6058. (b) Terao, T.; Miura, H.; Saika, A. *J. Chem. Phys.* **1986**, *85*, 3816−3826.

(22) (a) Wu, C. H.; Ramamoorthy, A.; Opella, S. *J. Magn. Reson.* **1994**, *A109*, 270−272. (b) Ramamoorthy, A.; Opella, S. *J. Solid State NMR Spectrosc.* **1995**, *4*, 387−392.

(23) Ramamoorthy, A.; Gierasch, L. M.; Opella, S. J. *J. Magn. Reson.* **1996**, *B110*, 102−106.

(24) Nakai, T.; McDowell, C. A. *J. Am. Chem. Soc.* **1994**, *116*, 6373−6383.

(25) Ramamoorthy, A.; Wu, C. H.; Opella, S. J. *J. Magn. Reson.* **1995**, *B107*, 88−90.

(26) Opella, S. J.; Stewart, P. L.; Valentine, K. G. *Q. Rev. Biophys.* **1987**, *19*, 7−49.

(27) Cornell, B. A.; Separovic, F.; Smith, R. In *Transport Through Membranes: Carriers, Channels and Pumps*; Pullman, A., Ed.; Kluwer Academic Publishers: Dordrecht, 1988; pp 289−295.

(28) Separovic, F.; Hayamizu, K.; Smith, R.; Cornell, B. A. *Chem. Phys. Lett.* **1991**, *181*, 157−162.

(29) Jardetzky, O.; Roberts, G. C. K. *NMR in Molecular Biology*; Academic Press: New York, 1981.

(30) Markley, J. L. *Acc. Chem. Res.* **1975**, *8*, 70.

(31) Frey, M. H.; Opella, S. J. *J. Magn. Reson.* **1986**, *66*, 144−147.

(32) Munowitz, M.; Bachovchin, W. W.; Herzfeld, J.; Dobson, C. M.; Griffin, R. G. *J. Am. Chem. Soc.* **1982**, *104*, 1192−1196.

(33) Huang, T.-H.; Bachovchin, W. W.; Griffin, R. G.; Dobson, C. M. *Biochemistry* **1984**, *23*, 5933−5937.

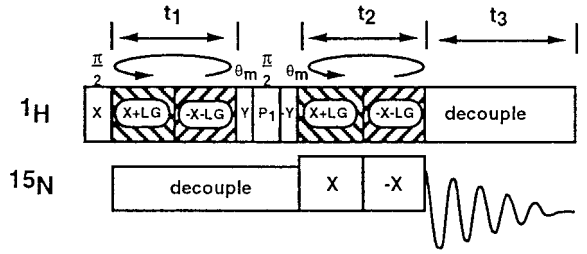

Figure 2. Schematic timing diagram of the three-dimensional pulse sequence that correlates the chemical shifts of I and S nuclei and the I−S coupling. Homonuclear I−I dipolar couplings are suppressed during t_1 and t_2 by the off-resonance flip−flop Lee−Goldburg (FFLG-2) pulse sequence. Heteronuclear I−S dipolar decoupling is accomplished with the continuous irradiation of S and I spins during t_1 and t_3 periods, respectively. In the t_2 period, I spin magnetization is selectively transferred to S via the I−S dipolar coupling. θ_m is a 54.7° pulse. Phase cycling is implemented for the spin-temperature alternation and the t_1 quadrature detection.

Single-crystal samples of tryptophan are not available for comparison. The histidine sample was prepared in the same way as the one used in the previous study.[15] The material was dissolved in water, then dilute HCl was added to reduce the pH from 7 to 2 to ensure that the $^{15}N_{\pi}$ site had a bonded hydrogen, and the final solution was lyophilized to generate the powder material used in the experiments. The isotropic chemical shift of the histidine powder sample was measured in a magic angle sample spinning experiment and found to be the same as that observed in the earlier experiments, demonstrating that all features of our sample were the same.

The pulse sequence for the three-dimensional solid-state NMR experiment that correlates the ^{1}H chemical shift, ^{1}H−^{15}N dipolar coupling, and ^{15}N chemical shift frequencies is diagramed in Figure 2.[5,25] The experimental parameters were optimized by using a single-crystal test sample, which allows ready measurement of line widths. The efficiency of the line narrowing of the flip−flop Lee−Goldburg multiple pulse sequence[34] in t_1 and t_2 and the selectivity of the coherence transfer from ^{1}H to ^{15}N during t_2 depend on the precise calibration of switched offset frequencies, radio frequency powers, cycle times, and synchronization of the phase and frequency jumps. Two-dimensional ^{1}H/^{15}N chemical shift correlation experiments were performed on the single-crystal test samples with interactive variation of these parameters to set up the three-dimensional experiments. In particular, the ^{1}H resonance line widths, which are very sensitive to the Lee−Goldburg conditions, were monitored and, at the same time, the experimental scaling factors were checked by measuring the frequency offsets of the ^{1}H spectral lines. Typically, ^{1}H line widths $\leq$0.8 ppm with scaling factors of 0.56 ± 0.02 were obtained. A two-dimensional experiment that correlates the ^{1}H−^{15}N dipolar coupling and ^{15}N chemical shift frequencies using the polarization inversion spin exchange at the magic angle (PISEMA) pulse sequence[22] gave a line width of 180 Hz in the dipolar dimension. The scaling factor of the PISEMA experiment was found to be 0.81 ± 0.01 by comparison with ^{1}H−^{15}N dipolar spectra obtained with separated local field spectroscopy without irradiation during t_1.

The experiments used were performed with radio frequency field strengths corresponding to 62.5 kHz and in a $\pi/2$ pulse width of 4 μs in both ^{1}H and ^{15}N radio frequency channels. An off-resonance frequency jump of 44.4 kHz was used to establish the Lee−Goldburg line-narrowing condition. During spin exchange at the magic angle (SEMA),[4,25] a 77 kHz radio frequency field was used in the ^{15}N radio frequency channel to match the effective field of the ^{1}H radio frequency channel. All measurements were made at room temperature. The ^{15}N frequencies were referenced to NH_3 (liquid, 25 °C) by setting the observed ^{15}N signal of solid $(^{15}NH_4)_2SO_4$ to 26.8 ppm. ^{1}H frequencies were referenced to tetramethylsilane by setting the observed ^{1}H signal of water (liquid, 25 °C) to 4.8 ppm. The data were processed on a Silicon Graphics Computer using the FELIX program (Biosym).

Calculations of the two-dimensional powder patterns corresponding to the correlations of ^{1}H chemical shift and ^{1}H−^{15}N dipolar coupling, ^{15}N chemical shift and ^{1}H−^{15}N dipolar coupling, and ^{1}H and ^{15}N chemical shift frequencies were carried out by using a Monte Carlo method to generate the orientations of the N−H bonds with respect to the external magnetic field.[2,5] 10^6 iterations were used for each powder pattern, and no significant change was observed with additional iterations. Experimentally measured principal values of the interactions and line widths were used in the respective simulated spectrum; further, the principal values were varied slightly to arrive at the best experimental and simulated spectral match. The principal components of the chemical shift tensors are represented according to the convention $|\sigma_{33}| \geq |\sigma_{22}| \geq |\sigma_{11}|$.

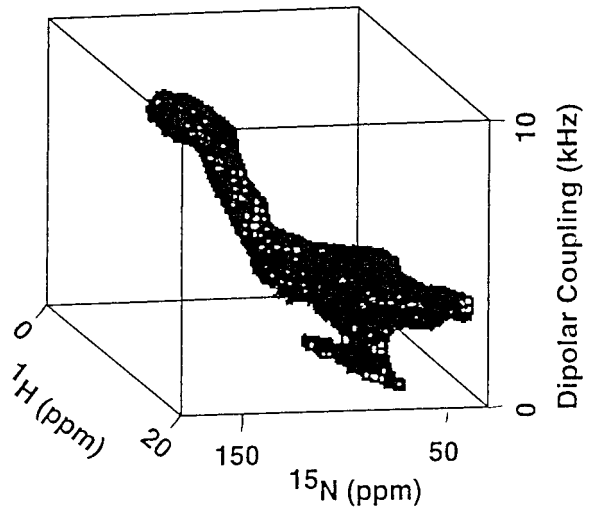

Figure 3. Three-dimensional ^{1}H shift/^{1}H−^{15}N coupling/^{15}N shift spectrum of the $^{15}N_{\epsilon 1}$-tryptophan powder sample. The three-dimensional spectrum was obtained by using the pulse sequence given in Figure 2. For this study 24 t_1 and 32 t_2 experiments with respective dwell times of 21.6 and 27 μs were performed, and 24 signal transients were coadded with a recycle delay of 5 s.

The one-dimensional ^{15}N chemical shift spectra of the labeled His and Trp samples are highly reproducible, enabling the magnitudes of the principal values of the chemical shift tensors to be determined within ±1 ppm. The isotropic chemical shift values determined from the average of the principal values and from magic angle sample spinning spectra are the same. More importantly, the magic angle spinning spectra displayed only a single narrow center, ruling out the presence of multiple crystal forms.

Two-dimensional PISEMA spectra are highly reproducible and are employed as part of the tune-up procedure for the three-dimensional experiments. As such, they were repeated more than twenty times for both samples and found to give the same results in the chemical shift and dipolar dimensions. Thus, uncertainties in the bond lengths and the orientations of the principal elements in the molecular frame arise from the comparison of the experimental and simulated spectra. We estimate that the errors in the determination of the magnitude of the dipolar couplings are approximately ±2 kHz leading to an uncertainty in the bond length of ±0.02 Å. $\beta_N = 0° \pm 2°$ based on many comparisons of experimental and simulated two-dimensional PISEMA powder patterns.

The experiments involving ^{15}N chemical shifts have greater errors than those with only the ^{1}H−^{15}N heteronuclear dipolar interactions. This is a consequence of the difficulty of narrowing the ^{1}H resonances, establishing the experimental scaling factor, and phasing the powder pattern spectra. As a result the ^{1}H chemical shift values have an uncertainty of ±1 ppm, and the angles (α_H and β_H) determined from these data have an uncertainty of ±4°. Also because of the influence of the ^{1}H chemical shift measurements, the uncertainties for the angles α_{NH} and β_{NH} are ±3° while that for γ_{NH} is ±4°.

Results

The three-dimensional spectrum of $^{15}N_{\epsilon 1}$-Trp in Figure 3 correlates the ^{1}H chemical shift, ^{1}H−^{15}N dipolar coupling, and ^{15}N chemical shift frequencies for all orientations of the

(34) Bielecki, A.; Kolbert, A. C.; de Groot, H. J. M.; Griffin, R. G.; Levitt, M. H. *Adv. Magn. Reson.* **1990**, *14*, 111−124.

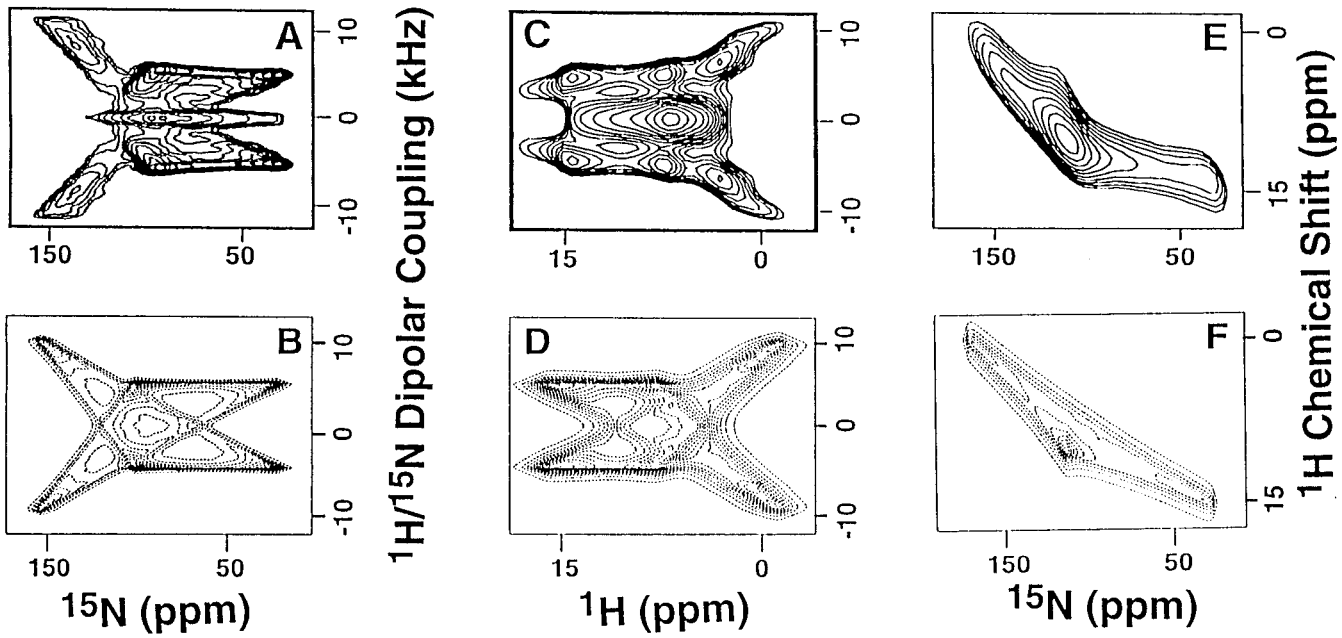

Figure 4. Comparison of experimental (top) and the best fitting simulated (bottom) two-dimensional spectra corresponding to orthogonal planes of the three-dimensional spectrum in Figure 3. (A, B) Correlations of ^{15}N shift and ^{1}H−^{15}N coupling; (C, D) correlations of ^{1}H shift and ^{1}H−^{15}N coupling; (E, F) correlations of ^{1}H shift and ^{15}N shift. Spectra C and E were obtained from the three-dimensional spectrum in Figure 3 by co-adding all the two-dimensional planes along the respective third dimension.

crystallites in the powder sample. The full frequency spans of both chemical shift interactions and the positive frequencies of the symmetric ^{1}H−^{15}N dipolar couplings, after adjustment for the relevant experimental scaling factors, are present in the spectrum in Figure 3. The overall appearance of this three-dimensional spectrum is diagnostic for the principal axes of the ^{1}H and ^{15}N chemical shift tensors being aligned with the N−H bond axis. Although three-dimensional powder patterns typically have striking appearances,[2,25] they are difficult to analyze quantitatively. In practice, quantitative analysis is best performed by using two-dimensional powder patterns because their spectral features are readily simulated and highly sensitive to the relative orientations of two of the tensors at a time. The experimental spectrum shown in Figure 4A was obtained by using the two-dimensional PISEMA experiment[22] since this yielded a somewhat less distorted powder pattern than could be obtained from the three-dimensional data in Figure 3. The two-dimensional spectra C and E in Figure 4 were obtained by adding together all of the two-dimensional planes along the appropriate third frequency axis of the three-dimensional data set shown in Figure 3. The calculated spectra B, D, and F in Figure 4 are the simulated best fit two-dimensional powder patterns. The angles defining the relative orientations of the tensors are shown in Figure 5.

The calculated powder patterns shown in Figure 4 are the ones selected to most closely match the corresponding experimental spectra from a panel of powder patterns generated with the interactive variation of the angles defining the orientations of the tensors and the magnitudes of the principal elements of the two chemical shift interactions and the ^{1}H−^{15}N dipolar coupling. Representative calculated two-dimensional powder patterns are shown in Figures 6−8. The magnitudes of the principal elements of the chemical shift interactions were measured initially by the comparison of one-dimensional experimental and calculated powder patterns, and then refined through detailed comparisons of spectral features found in the experimental and calculated two-dimensional powder patterns. The principal elements of the ^{15}N chemical shift tensor are σ_{11N} = 61 ppm, σ_{22N} = 129.6 ppm, and σ_{33N} = 180.8 ppm. The

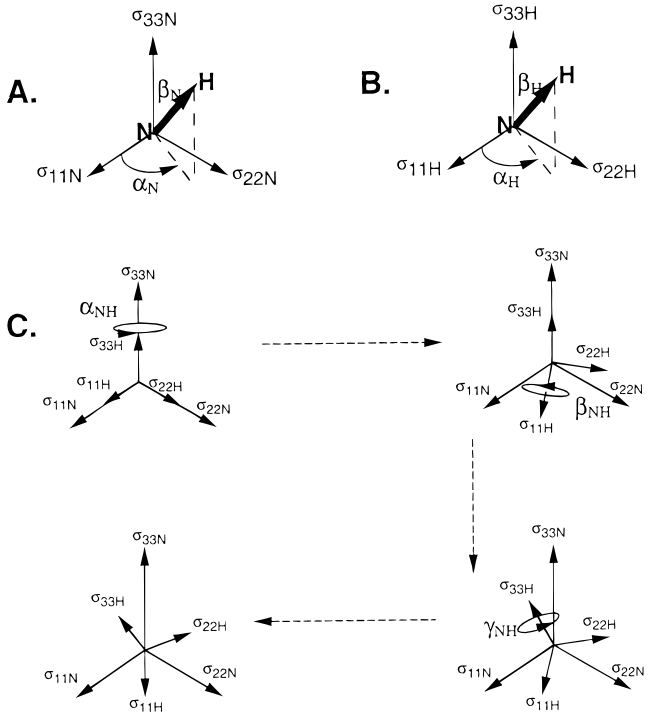

Figure 5. Orientations of the principal axes of the ^{15}N chemical shift (A) and ^{1}H chemical shift (B) tensors with respect to the N−H bond. α_i (i = N or H) is the angle between the σ_{11i} (i = N or H) and the projection of the N−H bond on the σ_{11i}−σ_{22i} plane. β_i (i = N or H) is the angle between the σ_{33i} and the N−H bond. Part C defines the unitary transformation between the principal coordinate systems of ^{1}H and ^{15}N chemical shifts. α_{NH}, β_{NH}, and γ_{NH} are the Euler angles.

principal elements of the ^{1}H chemical shift tensor are σ_{11H} = 0.4 ppm, σ_{22H} = 11 ppm, and σ_{33H} = 15 ppm. The maximum ^{1}H−^{15}N dipolar coupling directly measured from the one-dimensional ^{1}H−^{15}N dipolar spectral slice taken from the two-dimensional ^{15}N shift/^{1}H−^{15}N coupling and ^{1}H shift/^{1}H−^{15}N coupling experimental spectra is $D_{||}$ = 20.34 kHz.

The analysis of the experimental results in terms of orienta-

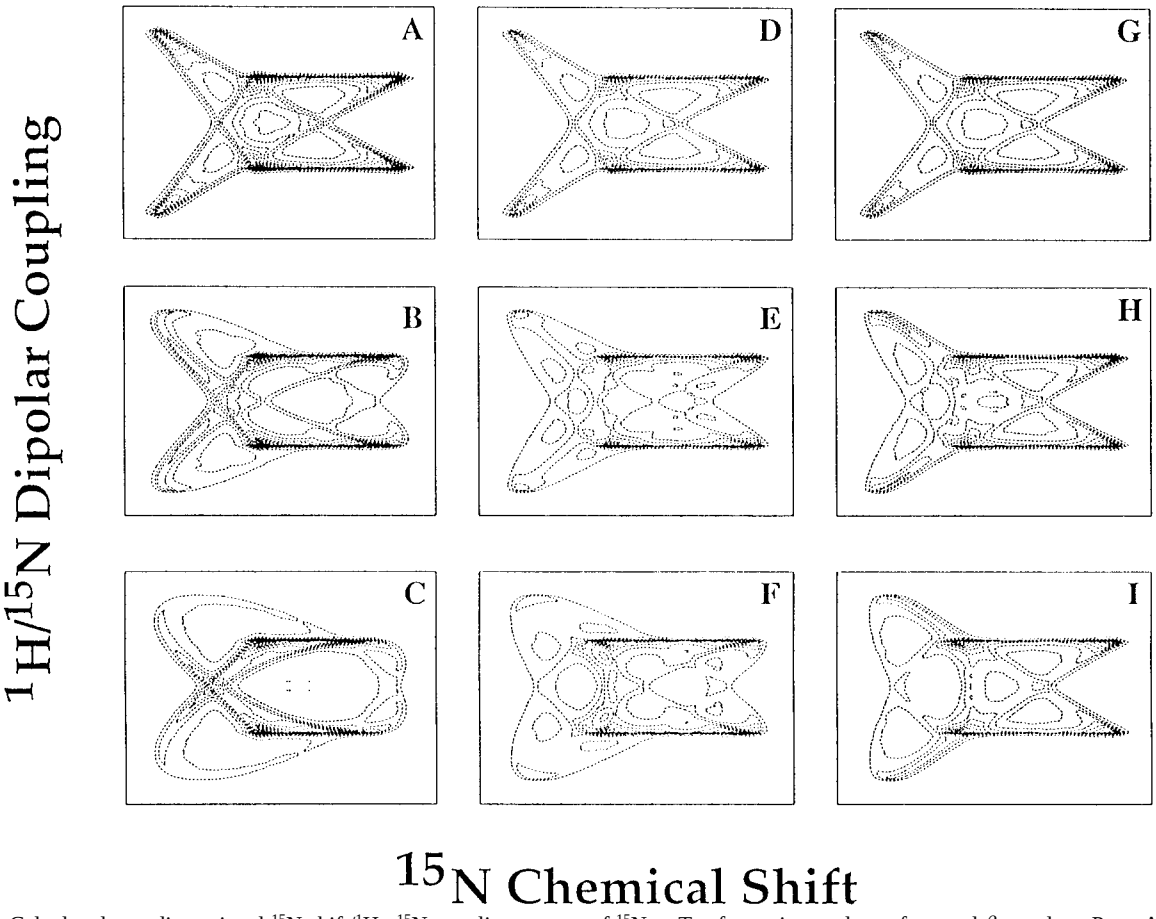

Figure 6. Calculated two-dimensional ^{15}N shift/$^{1}H-^{15}N$ coupling spectra of $^{15}N_{\epsilon 1}-$Trp for various values of α_N and β_N angles. Parts A, B, C, D, E, F, G, H, and I correspond to the (α_N,β_N) angles (0,0), (0,10), (0,20), (60,0), (60,10), (60,20), (90,0), (90,10), and (90,20), respectively.

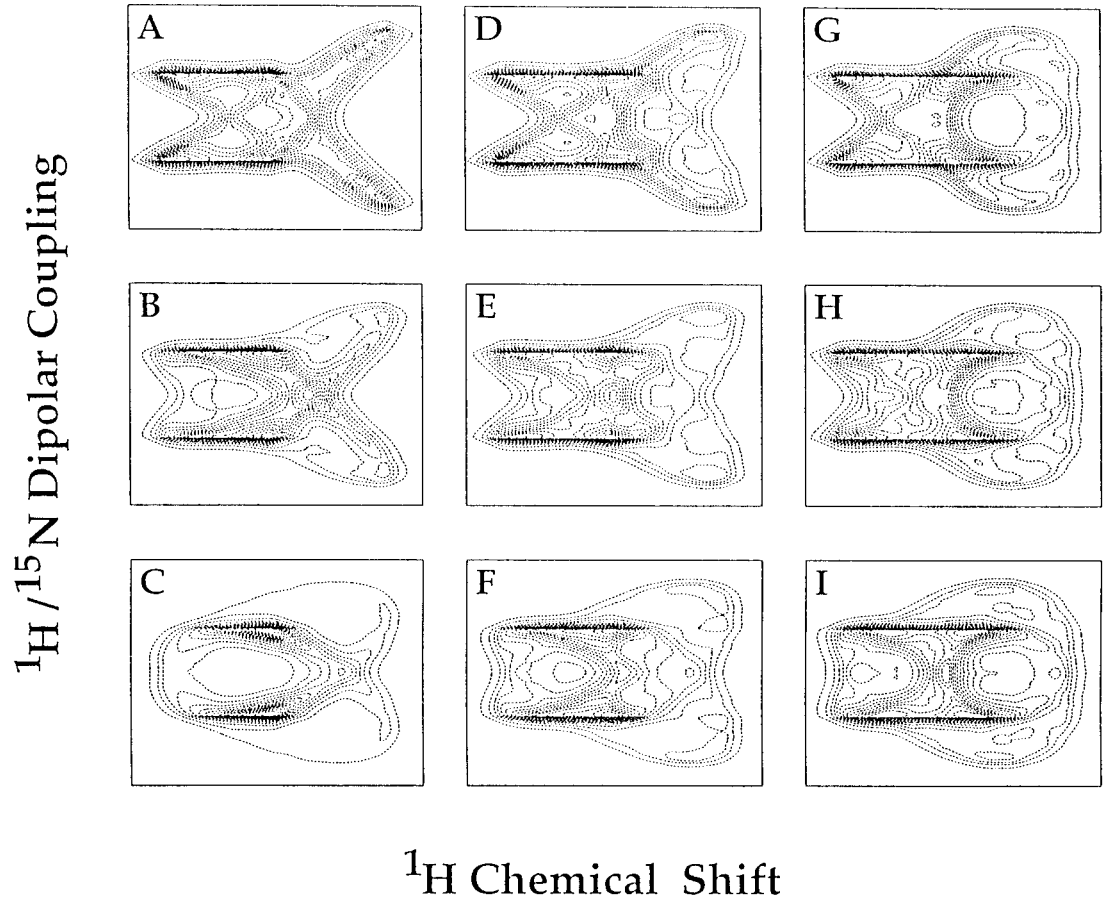

Figure 7. Calculated two-dimensional ^{1}H shift/$^{1}H-^{15}N$ coupling spectra of $^{15}N_{\epsilon 1}-$Trp for various values of α_H and β_H angles. Parts A, B, C, D, E, F, G, H, and I correspond to the (α_H,β_H) angles (0,90), (0,80), (0,70), (15,90), (15,80), (15,70), (30,90), (30,80), and (30,70), respectively.

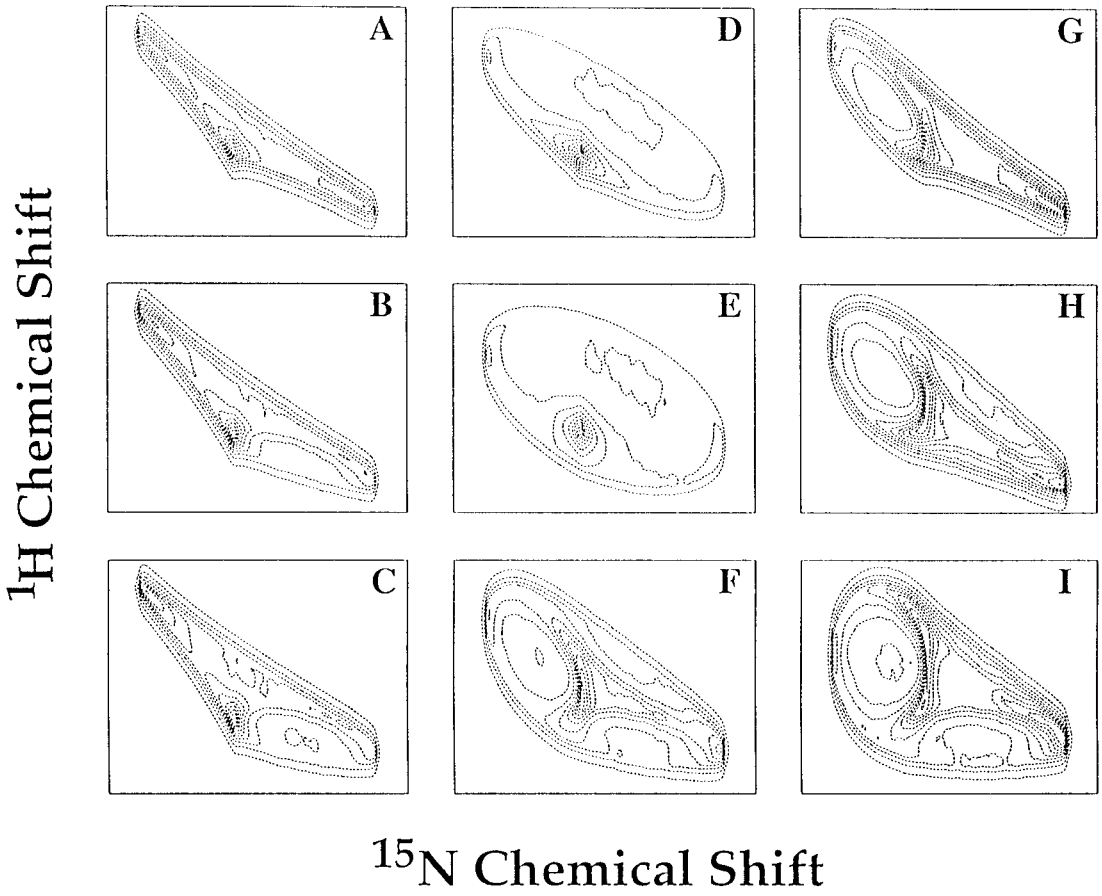

Figure 8. Calculated two-dimensional ^{1}H shift/^{15}N shift spectra of $^{15}N_{\epsilon 1}$−Trp for various values of α_{NH}, β_{NH}, and γ_{NH} angles. Parts A, B, C, D, E, F, G, H, and I correspond to the (α_{NH},β_{NH},γ_{NH}) angles (90,90,90), (80,90,90), (70,90,90), (90,80,90), (90,70,90), (80,80,80), (90,90,80), (90,90,70), and (70,70,70), respectively.

tions of the tensors in the molecular starts with the usual assumption that the axially symmetric ^{1}H−^{15}N dipolar interaction is colinear with the N−H bond.[5,8,12] This enables the relative orientations of the ^{1}H and ^{15}N chemical shift tensors determined from the spectra to be placed in the molecular frame of reference. The experimental data in Figure 4A are closely matched by the calculated powder pattern in Figure 4B with the angle $\beta_N = 0$. The simulations presented in Figure 6 show that the two-dimensional ^{15}N shift/^{1}H−^{15}N dipolar coupling powder pattern in Figure 4B is very sensitive to variation of the β_N angle. As a result the value of β_N is determined quite accurately. In contrast, the appearance of the simulated powder pattern does not change very much with variation of the α_N angle, as shown in Figure 6 (spectra A, D, and G). This is primarily because the projection of the N−H bond could be anywhere in the $\sigma_{22N}/\sigma_{11N}$ plane when $\beta_N = 0$; therefore, α_N can have any value. On the basis of the results in Figures 4C, 4D, and 7 we predict that β_H is 90°, where σ_{11H} is aligned along the N−H bond and α_H is 0°. Two-dimensional ^{1}H/^{15}N shift correlation powder patterns (Figures 4E, 4F, and 8) are best matched with values of the Euler angles $\alpha_{NH} = \beta_{NH} = \gamma_{NH} = 90°$. This confirms that σ_{33N} is colinear with σ_{11H} and the N−H bond, and that σ_{11N} is colinear with σ_{33H}. It also shows that σ_{22N} and σ_{22H} are pointing in opposite directions, and orthogonal to the $\sigma_{11i}/\sigma_{33i}$ (i = N or H) plane. Since these angles are given only with reference to the N−H bond, defining the complete orientation of the tensors in the molecular frame requires results from a single crystal of $^{15}N_\pi$-histidine, which has similar tensor orientations.[8,32] By incorporating this information in the analysis, σ_{22N} and σ_{22H} are found to be in the plane of the indole ring, and σ_{11N} and σ_{33H} are found to be orthogonal to the ring. The orientations of ^{1}H chemical shift and ^{15}N chemical shift

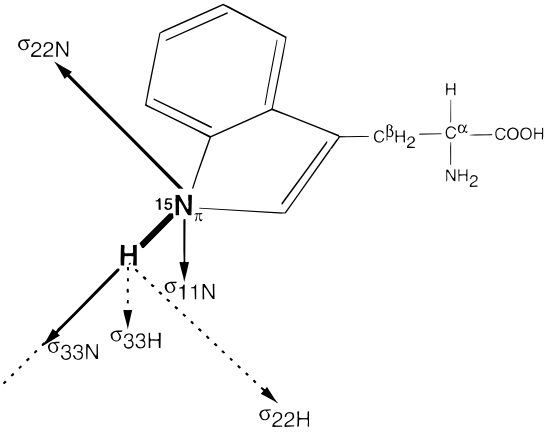

Figure 9. Orientations of the principal axes of ^{1}H chemical shift, ^{1}H−^{15}N dipolar, and ^{15}N chemical shift interaction tensors, pertaining to the indole ring $N_{\epsilon 1}$, in the molecular frame of tryptophan.

tensors are shown in the molecular frame of tryptophan in Figure 9. The properties of the tensor elements are summarized in Table 1.

The ^{1}H and ^{15}N tensors at the π site of histidine were also characterized by using the approach described above. The three-dimensional spectrum of $^{15}N_\pi$-His shown in Figure 10 resembles that of $^{15}N_{\epsilon 1}$-Trp in Figure 3. Two-dimensional spectra obtained from the three-dimensional data and relevant calculated spectra are shown in Figure 11. The orientations of the tensor elements are similar to those of the ^{15}N site of the indole in tryptophan; however, the magnitudes of principal elements of the shift tensors are significantly different. The magnitudes of the ^{1}H and ^{15}N chemical shift tensors, the ^{1}H−^{15}N dipolar coupling,

Table 1. Principal Components and Orientation of the ^1H Chemical Shift, $^1H-^{15}N$ Dipolar Coupling, and ^{15}N Chemical Shift Tensors of the $^{15}N_{\epsilon 1}$-Tryptophan Side Chain

$^{15}N/^1H-^{15}N$ parameters	$^1H/^1H-^{15}N$ parameters	$^1H/^{15}N$ parameters
$\sigma_{11N} = 61 \pm 1$ ppm	$\sigma_{11H} = 0.4 \pm 1$ ppm	$\alpha_{HN} = 88° \pm 2°$
$\sigma_{22N} = 129.6 \pm 1$ ppm	$\sigma_{22H} = 11 \pm 1$ ppm	$\beta_{HN} = 88° \pm 2°$
$\sigma_{33N} = 180.8 \pm 1$ ppm	$\sigma_{33H} = 15 \pm 1$ ppm	$\gamma_{HN} = 85° \pm 5°$
$\alpha_N = 0 \pm 30°$	$\alpha_H = 3 \pm 2°$	
$\beta_N = 5 \pm 3°$	$\beta_H = 88 \pm 2°$	

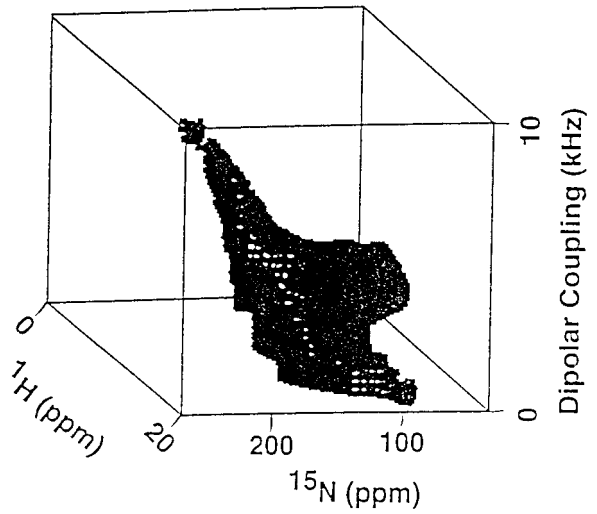

Figure 10. Three-dimensional ^1H chemical shift/$^1H-^{15}N$ dipolar coupling/^{15}N chemical shift correlation spectrum of the $^{15}N_{\pi}$-histidine powder sample obtained with use of the pulse sequence in Figure 2. For this study 20 t_1 and 24 t_2 experiments were performed with incremental times of 25.2 and 31.5 μs, respectively, and 80 ^{15}N signal transients were co-added with a recycle delay of 5 s.

and their orientations in the molecular frame are given in Table 2. The principal elements of the ^{15}N chemical shift tensor are $\sigma_{11N} = 77$ ppm, $\sigma_{22N} = 203$ ppm, and $\sigma_{33N} = 260$ ppm. The principal elements of the ^1H chemical shift tensor are $\sigma_{11H} = 0.3$ ppm, $\sigma_{22H} = 9.7$ ppm, and $\sigma_{33H} = 16.4$ ppm. The orientations of the tensors are shown in Figure 12. σ_{22i} (i = N or H), σ_{33N}, and σ_{11H} are in the plane of the imidazole ring. σ_{33N} and σ_{11H} are colinear with the N−H bond, and σ_{22N} and σ_{22H} point in the opposite directions. σ_{11N} and σ_{33H} are colinear, and are perpendicular to the plane of the ring. The ^{15}N chemical shift tensor determined from the analysis of the three-dimensional powder pattern is in good agreement with the previously reported results on L-histidine hydrochloride monohydrate by the single-crystal method.[8]

Discussion

Numerous ^{15}N, ^1H, and ^{13}C chemical shift tensors in amino acids and peptides have been characterized.[4,7−18] In addition, ab initio calculations[35,36] have been used to analyze the relationship between the polypeptide structure and chemical shifts of ^{15}N and ^{13}C nuclei. Three-dimensional experiments that simultaneously characterize the ^1H and ^{15}N chemical shift tensors have been applied to the amide N−H bond on various peptides and proteins[5,25] and give experimental results that are in agreement with previously reported studies.[14−18,26] Although the magnitudes of the principal components of these tensors differ somewhat among various amide fragments, their orientations in the molecular frame are similar. As a consequence, three-dimensional spectra of peptide bond systems are similar in appearance[5,25] with a low intensity "hole" in the spectrum indicating that at least one of the chemical shift tensors is not colinear with the N−H bond. The σ_{33N} axis typically points 15° to 25° away from the N−H bond, although in all cases examined[14−18] so far the σ_{11H} axis is colinear with the N−H bond.[5,14−18] This consistency could be attributed to the similarities in the electronic structure and molecular structure of the amide sites. The tensors related to the N−H bond in an aromatic ring fall in a separate category, and they are entirely different from those of the amide site N−H bond. For example, the orientations of the chemical shift tensors of $^{15}N_{\epsilon 1}$-tryptophan and $^{15}N_{\pi}$-histidine are similar to each other, but distinctly different from those of the amide sites. Since the three-dimensional spectra do not have a low intensity "hole", like that observed for amide sites, the ^1H and ^{15}N shift tensors are colinear with the N−H bond in both of these aromatic sites. This spectral difference must arise from differences in the intrinsic chemical bonding. In all cases, the length of the N−H bond measured directly from the $^1H-^{15}N$ dipolar coupling is found to be 1.06 ± 0.02 Å. This value is somewhat longer than the neutron diffraction results; however, it is in agreement with most of the previously reported solid-state NMR measurements.

The magnitudes of the principal elements of the ^{15}N-Trp chemical shift tensor found here agree well with previously reported results.[3,4] Cross and Opella[3] originally predicted that the σ_{33N} axis of $^{15}N_{\epsilon 1}$-Trp is colinar with the N−H bond on the basis of several chemical and spectropic arguments. Later, Hu et al.[4] analyzed the one-dimensional ^{15}N chemical shift powder pattern of $\{^{15}N_{\epsilon 1}-^2H\}$-Trp and reported that σ_{33N} points 25° away from the N−H bond. Hu et al.[4] used simultaneous optimization of the principal elements of ^{15}N chemical shift, $^{15}N-^2H$ dipolar, ^2H quadrupole interactions, and the angles defining the relative orientation of these tensors in their characterization of the tensors with one-dimensional dipolar−chemical shift spectroscopy. The complexity of this approach, especially where the dipolar coupled nucleus is quadrupolar, can lead to difficulties, since the high-field approximation ignores the quadrupole effects of the ^2H nuclei on the ^{15}N resonance. In contrast, two-dimensional PISEMA spectra[5,22] depend only on the N−H bond length, the magnitudes of the principal values of the chemical shift tensor, and the relative orientations of the chemical shift and heteronuclear dipolar interaction tensors. The principal elements of the ^{15}N shift tensor are directly measured by comparing the simulated and experimental one-dimensional ^{15}N powder patterns, and the magnitude of the $^1H-^{15}N$ dipolar coupling and its orientation are obtained independently from the two-dimensional ^1H shift/$^1H-^{15}N$ dipolar spectrum. As is evident from the spectra in Figure 6, a calculated ^{15}N shift/$^1H-^{15}N$ dipolar coupling powder pattern with $\beta_N = 0°$ matches as well with the experimental spectrum. Also, the $^1H/^{15}N$ chemical shift correlation spectrum separately predicts the relative orientations of the ^1H and ^{15}N chemical shift tensors. From these three independent experimental spectroscopic measurements, with the inclusion of all reasonable sources of experimental errors, we predict that the β_N angle is not greater than 4°. This finding is in agreement with the initial report of Cross and Opella,[3] but differs from that of Hu et al.[4] Our analysis of the relevant tensors at the $^{15}N_{\pi}$ site of histidine agrees well with the previously reported results from a single-crystal NMR study,[11] which further supports the accuracy of tensor determination from

(35) (a) Chesnut, D. B.; Phung, C. G. *Chem. Phys. Lett*. **1991**, *183*, 505−509. (b) Chesnut, D. B.; Phung, C. G. *Nuclear Magnetic Shielding and Molecular Structure*; NATO ASI Series C; Tossell, J. A., Ed.; Kluwer Academic Publishers: Dordrecht, 1993; Vol. 386, pp 221−241.

(36) (a) de Dios, A. C.; Pearson, J. G.; Oldfield, E. *Science* **1993**, *260*, 1491−1496. (b) de Dios, A. C.; Oldfield, E. *J. Am. Chem. Soc*. **1994**, *116*, 5307−5314.

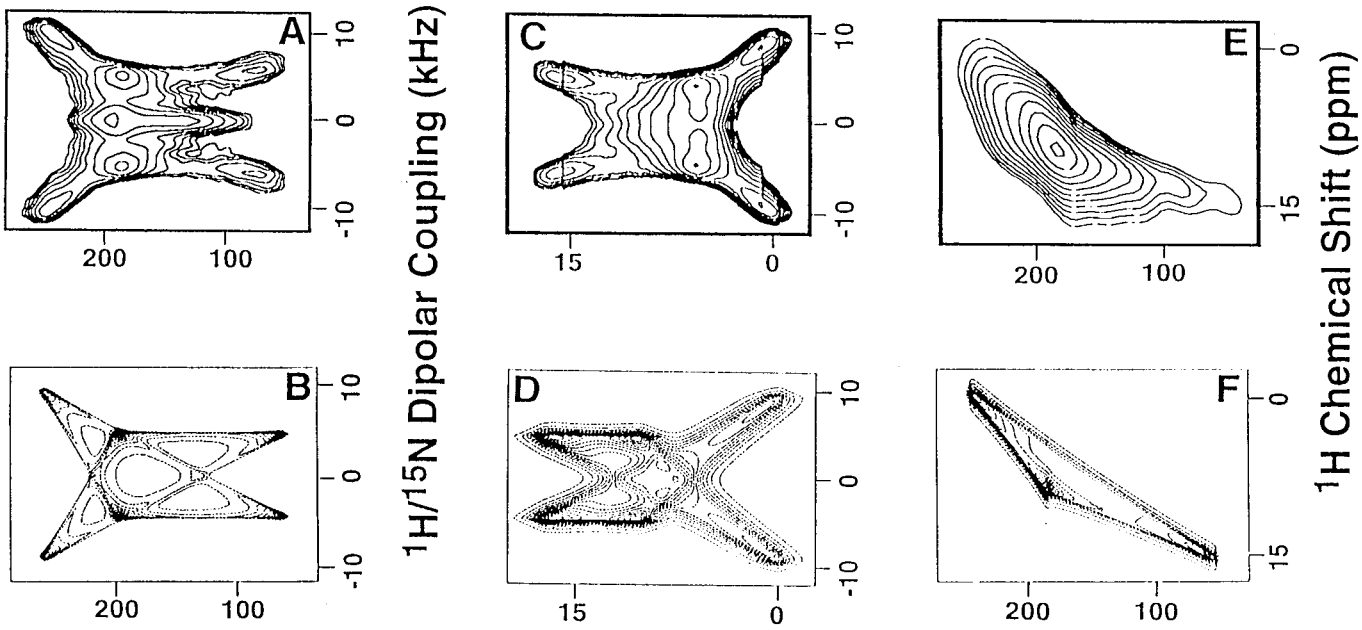

Figure 11. Comparison of experimental (top) and the best fitting calculated (bottom) two-dimensional spectra corresponding to orthogonal planes of the three-dimensional spectrum in Figure 10. (A, B) Correlations of ^{15}N shift and ^{1}H−^{15}N coupling; (C, D) correlations of ^{1}H shift and ^{1}H−^{15}N coupling; (E, F) correlations of ^{1}H shift and ^{15}N shift. Spectra C and E were obtained from the three-dimensional spectrum in Figure 10 by co-adding all the two-dimensional planes along the respective third dimension.

Table 2. Principal Components and Orientation of the ^{1}H Chemical Shift, ^{1}H−^{15}N Dipolar Coupling, and ^{15}N Chemical Shift Tensors of the $^{15}N_\pi$-Histidine Side Chain

^{15}N/^{1}H−^{15}N parameters	^{1}H/^{1}H−^{15}N parameters	^{1}H/^{15}N parameters
$\sigma_{11N} = 77 \pm 1$ ppm	$\sigma_{11H} = 0.3 \pm 1$ ppm	$\alpha_{HN} = 88° \pm 2°$
$\sigma_{22N} = 203 \pm 1$ ppm	$\sigma_{22H} = 9.7 \pm 1$ ppm	$\beta_{HN} = 88° \pm 2°$
$\sigma_{33N} = 260 \pm 1$ ppm	$\sigma_{33H} = 16.4 \pm 1$ ppm	$\gamma_{HN} = 85° \pm 5°$
$\alpha_N = 0 \pm 30°$	$\alpha_H = 3 \pm 2°$	
$\beta_N = 5 \pm 3°$	$\beta_H = 88 \pm 2°$	

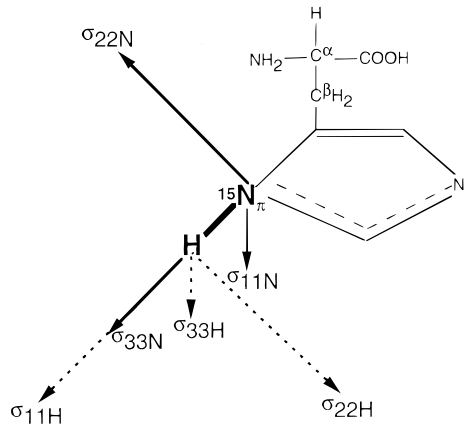

Figure 12. Orientations of the principal axes of ^{1}H chemical shift, ^{1}H−^{15}N dipolar, and ^{15}N chemical shift interaction tensors, pertaining to the imidazole ring N_π, in the molecular frame of histidine.

three-dimensional correlation spectra of powder samples, in general, and the finding that σ_{33N} is colinear with the N−H band in the side chain of tryptophan, in particular.

The three-dimensional correlation experiment avoids the necessity of preparing a single-crystal sample to determine chemical shift tensors. Since the spectral frequencies from each spin interaction are selectively measured in separate dimensions of the three-dimensional spectrum, the results are accurate. An important feature of the three-dimensional spectrum is the measurement of the local field through the correlation of ^{1}H chemical shift and ^{1}H−^{15}N dipolar couplings. This allows the measurement of the principal elements of the ^{1}H chemical shift tensor directly from the one-dimensional powder pattern and its orientation with respect to the N−H bond in the molecular frame. This is, in effect, the ^{1}H separated local field spectrum. Such information was previously available only through complex experiments on single crystals.[10,13] Approximately 10 mg of a molecule labeled in a single site with ^{15}N is needed for full characterization of the tensors in stationary samples, using the approach described here. However, the tensors from multiple sites can be resolved with the simple mention of magic angle turning versions of these experiments.[23] By eliminating the need for single-crystal samples, the chemical shift tensors in previously inaccessible sites can be characterized. This will have a substantial impact on the analysis of both solid-state NMR and solution NMR data for a wide range of chemical and biological systems.

Acknowledgment. This research was supported by Grant Nos. R37 GM24266 and RO1 GM29754 from the General Medical Sciences Institute, National Institutes of Health, and utilized the Resource for Solid-State NMR of Proteins at the University of Pennsylvania: An NIH Supported Research Center, supported by Grant No. P41 RR097393, from the Biomedical Research Technology Program, National Center for Research Resources, National Institutes of Health.

JA9632670